

# $\eta_c$ photoproduction at LHC energies

V. P. Gonçalves and B. D. Moreira

*High and Medium Energy Group,  
Instituto de Física e Matemática,  
Universidade Federal de Pelotas*

*Caixa Postal 354, CEP 96010-900, Pelotas, RS, Brazil*

(Dated: November 9, 2018)

In this contribution, we study the inclusive and diffractive  $\eta_c$  photoproduction in  $pp$  and  $pPb$  ultra-peripheral collisions (UPC's) at the LHC Run 2 energies. The quarkonium production is studied using nonrelativistic quantum chromodynamics (NRQCD) formalism. We present predictions for rapidity and transverse momentum distributions for the  $\eta_c$  photoproduction and present our estimate for the total cross sections at the Run 2 energies.

PACS numbers: 12.38.-t; 13.60.Le; 13.60.Hb

Keywords: Ultrapерipheral Heavy Ion Collisions,  $\eta_c$  Photoproduction, Nonrelativistic Quantum Chromodynamics.

## I. INTRODUCTION

In a hadron-hadron UPC, it is well known that the hadrons can act as sources of almost real photons allowing the study of photon-photon and photon-hadron interactions (the photon-induced processes) [1]. Our goal in this contribution is the study of the  $\eta_c$  production in the photon-gluon and the photon-Pomeron subprocesses, as shown in Fig.1, using the nonrelativistic QCD formalism (NRQCD). In this formalism, the photon-hadron process can be factorized in terms of the short distance coefficients for the photon-gluon subprocess (perturbatively calculated) and long distance matrix elements, related to the formation of the quarkonium at the final state, which are extracted from global analysis of the quarkonium data [2, 3]. As the photoproduction of  $\eta_c$  is a purely color octet contribution [2], this process is a probe of the color octet mechanism. In our analysis, we present our predictions for the rapidity and  $p_T$  distributions and total cross sections for the  $\eta_c$  photoproduction. A comparison with the predictions for the  $\eta_c$  production in photon-photon and exclusive photon-hadron interactions also is presented.

This contribution is organized as follows. In the next section we present the formalism to study the  $\eta_c$  photoproduction at hadron-hadron collisions, presenting a brief summary on the equivalent photon approximation and NRQCD. In Section III, we summarize our results for rapidity and  $p_t$  distributions and total cross sections. A more detailed discussion is presented in Ref.[4]. Lastly, in Section IV, we present our conclusions.

## II. $\eta_c$ PRODUCTION AT PHOTO-INDUCED PROCESSES

Let us consider an ultraperipheral collision (impact parameter  $> R_{h_1} + R_{h_2}$ ) between two fast hadrons. In this regime we can factorize the cross section for the  $\eta_c$  production in  $hh$  collisions in terms of the equivalent flux of photons of the hadron projectile and the photon-hadron cross section. The rapidity distribution for quarkonium photoproduction in hadron-hadron collisions is given by [4]

$$\frac{d\sigma_{hh}}{dY}(Y) = n_{h_1}(Y)\sigma_{\gamma h_2}(Y) + (1 \longleftrightarrow 2; Y \rightarrow -Y) \quad (1)$$

where the rapidity variable is related with the photon energy by  $Y = \ln(2\omega/M_{\eta_c})$  and  $n(Y)$  is the photon spectrum associated to the proton or nucleus which is dependent of the choice of the form factor. For protons as source of photons we use the dipole form factor, which leads to [5]

$$n_p(\omega) = \frac{\alpha_{em}}{2\pi} \left[ 1 + \left( 1 - \frac{2\omega}{\sqrt{s_{NN}}} \right)^2 \right] \left( \ln \Omega - \frac{11}{6} + \frac{3}{\Omega} - \frac{3}{2\Omega^2} + \frac{1}{3\Omega^3} \right), \quad (2)$$

where  $\Omega = 1 + [(0.71 \text{ GeV}^2)/Q_{\min}^2]$  and  $Q_{\min}^2 = \omega^2/[\gamma_L^2(1 - 2\omega/\sqrt{s})] \approx (\omega/\gamma_L)^2$ , where  $\gamma_L$  is the Lorentz boost of a single beam. For  $Pb$  we have used the hard sphere form factor, which gives the following photon flux [1]

$$n_A(\omega) = \frac{2Z^2\alpha_{em}}{\pi} \left[ \bar{\eta} K_0(\bar{\eta}) K_1(\bar{\eta}) - \frac{\bar{\eta}^2}{2} \mathcal{U}(\bar{\eta}) \right] \quad (3)$$

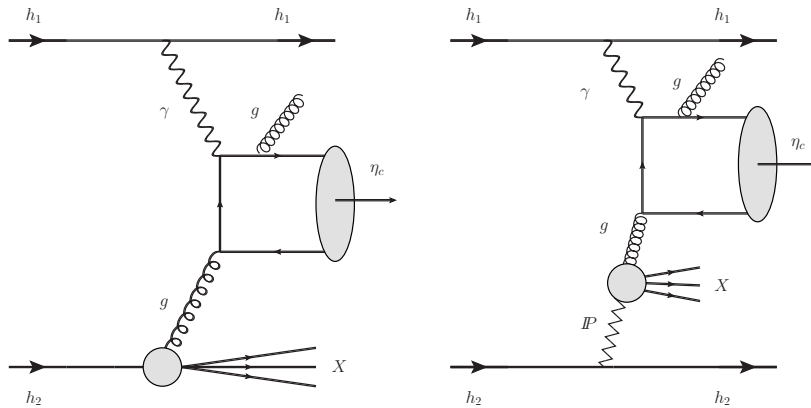


FIG. 1: Schematic view of diagrams for the inclusive (left) and diffractive (right)  $\eta_c$  production in hadronic collisions considering photon - hadron interactions.

where  $K_0(\eta)$  and  $K_1(\eta)$  are the modified Bessel functions,  $\bar{\eta} = \omega (R_{h_1} + R_{h_2})/\gamma_L$  and  $\mathcal{U}(\bar{\eta}) = K_1^2(\bar{\eta}) - K_0^2(\bar{\eta})$ .

In order to study the inelastic  $\eta_c$  photoproduction in the process  $\gamma + p \rightarrow \eta_c + X$ , we will use the NRQCD formalism, which allows us to factorize the subprocess  $\gamma + g \rightarrow \eta_c + g$  in two different steps: (i) the heavy pair production (perturbative), and (ii) the  $\eta_c$  formation, which is a nonperturbative process (see Fig. 1). Firstly, for the inclusive process  $\gamma + p \rightarrow \eta_c + X$  the cross section is given by [2, 4]

$$\sigma(\gamma + h \rightarrow \eta_c + X) = \int dz dp_T^2 \frac{xg(x, Q^2)}{z(1-z)} \frac{d\sigma}{dt}(\gamma + g \rightarrow \eta_c + g) \quad (4)$$

where  $z \equiv (p_{\eta_c} \cdot p)/(p_\gamma \cdot p)$  (fraction of the photon energy carried away by the  $\eta_c$  in the hadron rest frame), with  $p_{\eta_c}$ ,  $p$  and  $p_\gamma$  being the four momentum of the  $\eta_c$ , hadron and photon, respectively.  $p_T$  is the magnitude of the  $\eta_c$  transverse momentum and  $g(x, Q^2)$  is the standard gluon distribution function, which will be modelled using the CTEQ6LO parametrization [6] assuming that  $Q^2 = 4m_c^2$ . For the diffractive case we have used the diffractive gluon PDF derived by the H1 collaboration in Ref.[7]. The integration limits are taken so that  $z < 1$  and  $p_T^2 \geq 1 \text{ GeV}^2$ . The associated partonic differential cross section  $d\sigma/d\hat{t}$  is given by (see Ref.[2])

$$\frac{d\sigma}{d\hat{t}} = \frac{1}{16\pi\hat{s}^2} F^{(2S+1)L_J^{[8]}} \times \langle \mathcal{O}^{(2S+1)L_J^{[8]}} \rangle, \quad (5)$$

with the short distance coefficients  $F$  of the subprocesses being given by [2]

$$F(^3S_1^{[8]}) = 20(4\pi)^3 \alpha\alpha_S^2 e_c^2 M \frac{\mathcal{P}^2 - M^2 \hat{s}\hat{t}\hat{u}}{9Q^2} \quad (6)$$

$$F(^1S_0^{[8]}) = 3(4\pi)^3 \alpha\alpha_S^2 e_c^2 \hat{s}\hat{u} \frac{M^8 + \hat{s}^4 + \hat{t}^4 + \hat{u}^4}{M\hat{t}Q^2} \quad (7)$$

$$F(^1P_1^{[8]}) = \frac{80(4\pi)^3 \alpha\alpha_S^2 e_c^2}{9MQ^3} [M^2 Q (M^6 + 5\hat{s}\hat{t}\hat{u} - Q) - 2\hat{s}\hat{t}\hat{u} (\mathcal{P}^2 + 2M^8 - M^2 \hat{s}\hat{t}\hat{u})], \quad (8)$$

and

$$\mathcal{P} = \hat{s}\hat{t} + \hat{t}\hat{u} + \hat{s}\hat{u}, \quad (9)$$

$$\mathcal{Q} = (\hat{s} + \hat{t})(\hat{s} + \hat{u})(\hat{t} + \hat{u}). \quad (10)$$

Moreover,  $\langle \mathcal{O}^{(2S+1)L_J^{[8]}} \rangle$  are the long distance matrix elements, obtained from experimental data of the quarkonium production. Here we have used the updated values from Ref.[3].

### III. RESULTS

In the Figure 2 we present our predictions for the rapidity distribution ( $pp$  at  $\sqrt{s} = 13 \text{ TeV}$  and  $pA$  at  $\sqrt{s} = 8.1 \text{ TeV}$ ). As expected, the rapidity distributions in  $pp$  collisions are symmetric in  $Y = 0$ , while in the  $pA$  case are

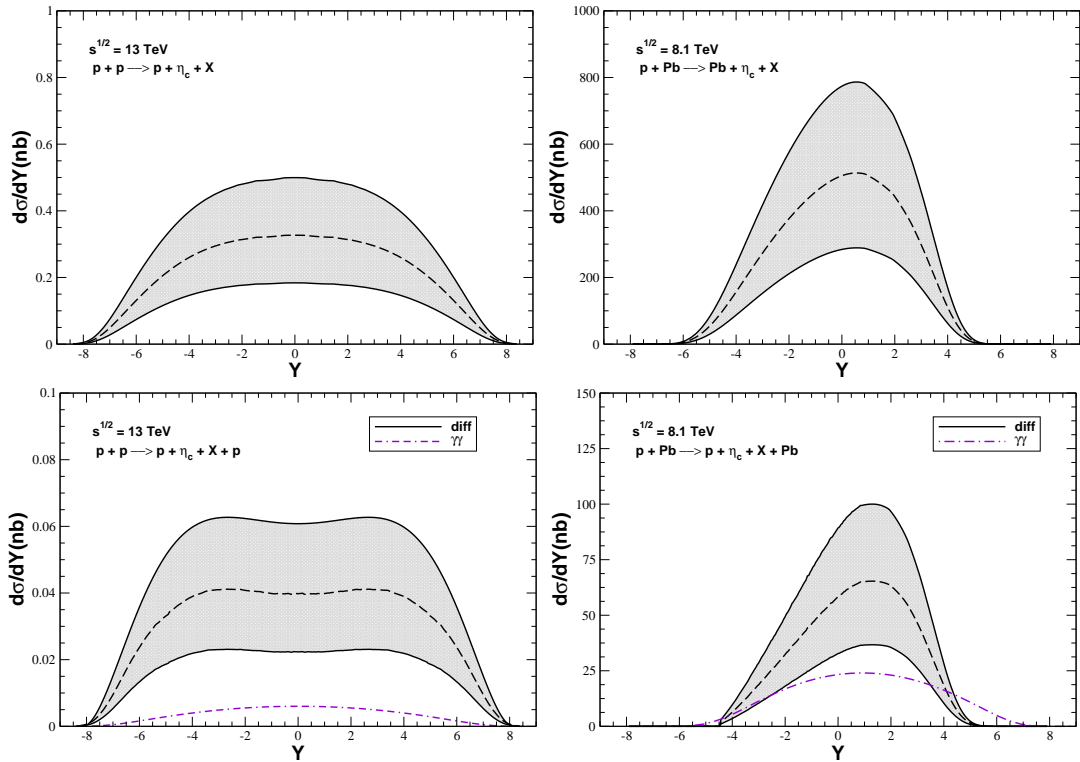


FIG. 2: Rapidity distribution for the  $\eta_c$  photoproduction. Upper row: inclusive photoproduction in  $pp$  collisions (left panel) and  $pA$  collisions (right panel). Lower row: diffractive photoproduction in  $pp$  collisions (left panel) and  $pA$  collisions (right panel).

asymmetric because of the dominance of the  $\gamma p$  interactions when the nucleus is acting as a source of photons. The bands presented are due to the uncertainty of the long distance matrix elements (Ref.[3]). Moreover, the inclusive production is about 10 times larger than the diffractive production. For the diffractive cases we present also the  $\gamma\gamma$   $\eta_c$  photoproduction, from Ref.[4].

In Fig. 3 we present the transverse momentum distributions for  $\eta_c$  photoproduction at  $Y = 0$  and  $\sqrt{s} = 13$  TeV. The dashed lines represent the inclusive case and the dot-dashed lines the diffractive case. As in Figure 2, we can observe that the inclusive case is about 10 times larger than the diffractive case. Moreover, we can observe that the behavior of distribution is  $1/p_t^n$ , which is a typical DGLAP behavior.

In the Table 1 we present our predictions for the total cross sections for the  $\eta_c$  photoproduction. For comparison, we present the predictions for the  $\eta_c$  photoproduction due to  $\gamma\gamma$  and  $\gamma\mathcal{D}$  mechanisms, from Refs.[4, 8]. As can be observed, the  $\gamma p$  inclusive mechanism is the dominant mechanism for the  $\eta_c$  photoproduction. Here it is important to emphasize that the  $\gamma P$  diffractive, the  $\gamma\gamma$  and the  $\gamma\mathcal{D}$  processes are characterized by two rapidity gaps at the final state. Furthermore, for the  $\gamma\mathcal{D}$  mechanism we have the smaller cross sections.

	$\gamma p$ inclusive	$\gamma P$ diffractive	$\gamma\gamma$ exclusive	$\gamma\mathcal{D}$ exclusive
$pp$ ( $\sqrt{s} = 13$ TeV)	3.492 nb	0.501 nb	0.059 nb	0.013 nb
$pPb$ ( $\sqrt{s} = 8.1$ TeV)	3.194 $\mu\text{b}$	0.351 $\mu\text{b}$	0.182 $\mu\text{b}$	0.032 $\mu\text{b}$

TABLE I: Total cross section for the  $\eta_c$  photoproduction. Here we also present the  $\eta_c$  production due to  $\gamma\gamma$  and  $\gamma\mathcal{D}$  mechanisms from Refs.[4, 8]

#### IV. CONCLUSIONS

The photo-induced processes at LHC have been a powerful tool to study the hadronic structure and the QCD dynamics in different processes. In this contribution, we have studied the  $\eta_c$  photoproduction in the NRQCD formalism.

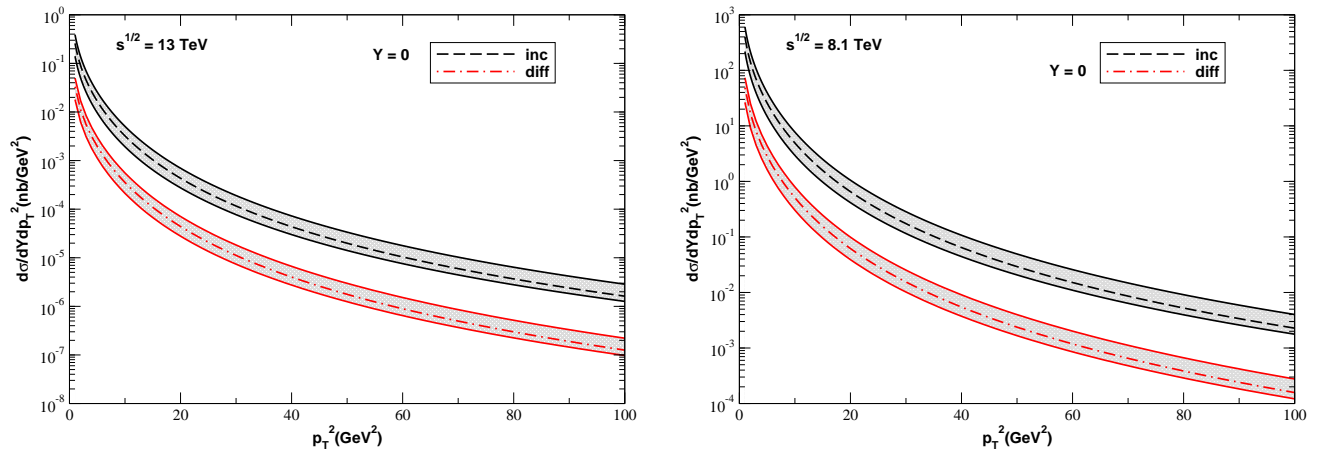


FIG. 3: Transverse momentum distributions for the inclusive and diffractive  $\eta_c$  photoproduction at central rapidities ( $Y = 0$ ) in  $pp$  collisions at  $\sqrt{s} = 13$  TeV (left panel) and  $pPb$  collisions at  $\sqrt{s} = 8.1$  TeV (right panel).

Following the Ref.[2], this process is a pure color octet and, therefore, it is a probe of the color octet mechanism. Moreover, it is important to note that the diffractive,  $\gamma\gamma$  and  $\gamma$ -Odderon mechanisms are characterized by two rapidity gaps at the final state. In particular, the detection of the exclusive ( $\gamma$ -Odderon) mechanism would be a direct probe of the perturbative Odderon. Since the diffractive and  $\gamma\gamma$  processes are backgrounds for the  $\gamma$ -Odderon process, the knowledge of their magnitudes can be useful for experimental analysis. Finally, the magnitude of the cross sections presented here, show that this study is feasible at LHC energies.

#### Acknowledgements

This work was partially financed by the Brazilian funding agencies CNPq, CAPES, FAPERGS and INCT-FNA (process number 464898/2014-5).

- 
- [1] G. Baur, K. Hencken, D. Trautmann, S. Sadovsky, Y. Kharlov, Phys. Rep. **364**, 359 (2002); V. P. Goncalves and M. V. T. Machado, Mod. Phys. Lett. A **19**, 2525 (2004); C. A. Bertulani, S. R. Klein and J. Nystrand, Ann. Rev. Nucl. Part. Sci. **55**, 271 (2005); K. Hencken *et al.*, Phys. Rept. **458**, 1 (2008).
  - [2] L. K. Hao, F. Yuan and K. T. Chao, Phys. Rev. Lett. **83**, 4490 (1999).
  - [3] G. M. Yu, Y. B. Cai, Y. D. Li and J. S. Wang, Phys. Rev. C **95**, no. 1, 014905 (2017) Addendum: [Phys. Rev. C **95**, no. 6, 069901 (2017)].
  - [4] V. P. Goncalves and B. D. Moreira, arXiv:1801.10501 [hep-ph].
  - [5] M. Drees and D. Zeppenfeld, Phys. Rev. D **39**, 2536 (1989).
  - [6] J. Pumplin, D. R. Stump, J. Huston, H. L. Lai, P. M. Nadolsky and W. K. Tung, JHEP **0207**, 012 (2002).
  - [7] H1 Collab., A. Aktas *et al.*, Eur. Phys. J. **C48** (2006) 715.
  - [8] V. P. Goncalves, Nucl. Phys. A **902**, 32 (2013).